Multiple jet production at low transverse energies in $p\bar{p}$ collisions at $\sqrt{s}=1.8$ TeV

V. M. Abazov,[22] B. Abbott,[56] A. Abdesselam,[11] M. Abolins,[49] V. Abramov,[25] B. S. Acharya,[17] D. L. Adams,[54] M. Adams,[36] S. N. Ahmed,[21] G. D. Alexeev,[22] A. Alton,[48] G. A. Alves,[2] E. W. Anderson,[41] Y. Arnoud,[9] C. Avila,[5] V. V. Babintsev,[25] L. Babukhadia,[53] T. C. Bacon,[27] A. Baden,[45] B. Baldin,[35] P. W. Balm,[20] S. Banerjee,[17] E. Barberis,[29] P. Baringer,[42] J. Barreto,[2] J. F. Bartlett,[35] U. Bassler,[12] D. Bauer,[27] A. Bean,[42] F. Beaudette,[11] M. Begel,[52] A. Belyaev,[34] S. B. Beri,[15] G. Bernardi,[12] I. Bertram,[26] A. Besson,[9] R. Beuselinck,[27] V. A. Bezzubov,[25] P. C. Bhat,[35] V. Bhatnagar,[15] M. Bhattacharjee,[53] G. Blazey,[37] F. Blekman,[20] S. Blessing,[34] A. Boehnlein,[35] N. I. Bojko,[25] T. A. Bolton,[43] F. Borcherding,[35] K. Bos,[20] T. Bose,[51] A. Brandt,[58] R. Breedon,[30] G. Briskin,[57] R. Brock,[49] G. Brooijmans,[35] A. Bross,[35] D. Buchholz,[38] M. Buehler,[36] V. Buescher,[14] V. S. Burtovoi,[25] J. M. Butler,[46] F. Canelli,[52] W. Carvalho,[3] D. Casey,[49] Z. Casilum,[53] H. Castilla-Valdez,[19] D. Chakraborty,[37] K. M. Chan,[52] S. V. Chekulaev,[25] D. K. Cho,[52] S. Choi,[33] S. Chopra,[54] J. H. Christenson,[35] D. Claes,[50] A. R. Clark,[29] L. Coney,[40] B. Connolly,[34] W. E. Cooper,[35] D. Coppage,[42] S. Crépé-Renaudin,[9] M. A. C. Cummings,[37] D. Cutts,[57] G. A. Davis,[52] K. De,[58] S. J. de Jong,[21] M. Demarteau,[35] R. Demina,[43] P. Demine,[9] D. Denisov,[35] S. P. Denisov,[25] S. Desai,[53] H. T. Diehl,[35] M. Diesburg,[35] S. Doulas,[47] Y. Ducros,[13] L. V. Dudko,[24] S. Duensing,[21] L. Duflot,[11] S. R. Dugad,[17] A. Duperrin,[10] A. Dyshkant,[37] D. Edmunds,[49] J. Ellison,[33] J. T. Eltzroth,[58] V. D. Elvira,[35] R. Engelmann,[53] S. Eno,[45] G. Eppley,[60] P. Ermolov,[24] O. V. Eroshin,[25] J. Estrada,[52] H. Evans,[51] V. N. Evdokimov,[25] D. Fein,[28] T. Ferbel,[52] F. Filthaut,[21] H. E. Fisk,[35] Y. Fisyak,[54] E. Flattum,[35] F. Fleuret,[12] M. Fortner,[37] H. Fox,[38] S. Fu,[51] S. Fuess,[35] E. Gallas,[35] A. N. Galyaev,[25] M. Gao,[51] V. Gavrilov,[23] R. J. Genik II,[26] K. Genser,[35] C. E. Gerber,[36] Y. Gershtein,[57] R. Gilmartin,[34] G. Ginther,[52] B. Gómez,[5] P. I. Goncharov,[25] H. Gordon,[54] L. T. Goss,[59] K. Gounder,[35] A. Goussiou,[27] N. Graf,[54] P. D. Grannis,[53] J. A. Green,[41] H. Greenlee,[35] Z. D. Greenwood,[44] S. Grinstein,[1] L. Groer,[51] S. Grünendahl,[35] A. Gupta,[17] S. N. Gurzhiev,[25] G. Gutierrez,[35] P. Gutierrez,[56] N. J. Hadley,[45] H. Haggerty,[35] S. Hagopian,[34] V. Hagopian,[34] R. E. Hall,[31] S. Hansen,[35] J. M. Hauptman,[41] C. Hays,[51] C. Hebert,[42] D. Hedin,[37] J. M. Heinmiller,[36] A. P. Heinson,[33] U. Heintz,[46] M. D. Hildreth,[40] R. Hirosky,[61] J. D. Hobbs,[53] B. Hoeneisen,[8] Y. Huang,[48] I. Iashvili,[33] R. Illingworth,[27] A. S. Ito,[35] M. Jaffré,[11] S. Jain,[17] R. Jesik,[27] K. Johns,[28] M. Johnson,[35] A. Jonckheere,[35] H. Jöstlein,[35] A. Juste,[35] W. Kahl,[43] S. Kahn,[54] E. Kajfasz,[10] A. M. Kalinin,[22] D. Karmanov,[24] D. Karmgard,[40] R. Kehoe,[49] A. Khanov,[43] A. Kharchilava,[40] S. K. Kim,[18] B. Klima,[35] B. Knuteson,[29] W. Ko,[30] J. M. Kohli,[15] A. V. Kostritskiy,[25] J. Kotcher,[54] B. Kothari,[51] A. V. Kozelov,[25] E. A. Kozlovsky,[25] J. Krane,[41] M. R. Krishnaswamy,[17] P. Krivkova,[6] S. Krzywdzinski,[35] M. Kubantsev,[43] S. Kuleshov,[23] Y. Kulik,[35] S. Kunori,[45] A. Kupco,[7] V. E. Kuznetsov,[33] G. Landsberg,[57] W. M. Lee,[34] A. Leflat,[24] C. Leggett,[29] F. Lehner,[35,*] C. Leonidopoulos,[51] J. Li,[58] Q. Z. Li,[35] J. G. R. Lima,[3] D. Lincoln,[35] S. L. Linn,[34] J. Linnemann,[49] R. Lipton,[35] A. Lucotte,[9] L. Lueking,[35] C. Lundstedt,[50] C. Luo,[39] A. K. A. Maciel,[37] R. J. Madaras,[29] V. L. Malyshev,[22] V. Manankov,[24] H. S. Mao,[4] T. Marshall,[39] M. I. Martin,[37] A. A. Mayorov,[25] R. McCarthy,[53] T. McMahon,[55] H. L. Melanson,[35] M. Merkin,[24] K. W. Merritt,[35] C. Miao,[57] H. Miettinen,[60] D. Mihalcea,[37] C. S. Mishra,[35] N. Mokhov,[35] N. K. Mondal,[17] H. E. Montgomery,[35] R. W. Moore,[49] M. Mostafa,[1] H. da Motta,[2] Y. D. Mutaf,[53] E. Nagy,[10] F. Nang,[28] M. Narain,[46] V. S. Narasimham,[17] N. A. Naumann,[21] H. A. Neal,[48] J. P. Negret,[5] A. Nomerotski,[35] T. Nunnemann,[35] G. Z. Obrant,[63] D. O'Neil,[49] V. Oguri,[3] B. Olivier,[12] N. Oshima,[35] P. Padley,[60] K. Papageorgiou,[36] N. Parashar,[47] R. Partridge,[57] N. Parua,[53] A. Patwa,[53] O. Peters,[20] P. Pétroff,[11] R. Piegaia,[1] B. G. Pope,[49] E. Popkov,[46] H. B. Prosper,[34] S. Protopopescu,[54] M. B. Przybycien,[38,†] J. Qian,[48] R. Raja,[35] S. Rajagopalan,[54] P. A. Rapidis,[35] N. W. Reay,[43] S. Reucroft,[47] M. Ridel,[11] M. Rijssenbeek,[53] F. Rizatdinova,[43] T. Rockwell,[49] M. Roco,[35] C. Royon,[13] P. Rubinov,[35] R. Ruchti,[40] J. Rutherfoord,[28] B. M. Sabirov,[22] G. Sajot,[9] A. Santoro,[3] L. Sawyer,[44] R. D. Schamberger,[53] H. Schellman,[38] A. Schwartzman,[1] E. Shabalina,[36] R. K. Shivpuri,[16] D. Shpakov,[47] M. Shupe,[28] R. A. Sidwell,[43] V. Simak,[7] H. Singh,[33] V. Sirotenko,[35] P. Slattery,[52] R. P. Smith,[35] R. Snihur,[38] G. R. Snow,[50] J. Snow,[55] S. Snyder,[54] J. Solomon,[36] Y. Song,[58] V. Sorín,[1] M. Sosebee,[58] N. Sotnikova,[24] K. Soustruznik,[6] M. Souza,[2] N. R. Stanton,[43] G. Steinbrück,[51] R. W. Stephens,[58] D. Stoker,[32] V. Stolin,[23] A. Stone,[44] D. A. Stoyanova,[25] M. A. Strang,[58] M. Strauss,[56] M. Strovink,[29] L. Stutte,[35] A. Sznajder,[3] M. Talby,[10] W. Taylor,[53] S. Tentindo-Repond,[34] S. M. Tripathi,[30] T. G. Trippe,[29] A. S. Turcot,[54] P. M. Tuts,[51] V. Vaniev,[25] R. Van Kooten,[39] N. Varelas,[36] L. S. Vertogradov,[22] F. Villeneuve-Seguier,[10] A. A. Volkov,[25] A. P. Vorobiev,[25] H. D. Wahl,[34] H. Wang,[38] Z.-M. Wang,[53] J. Warchol,[40] G. Watts,[62] M. Wayne,[40] H. Weerts,[49] A. White,[58] J. T. White,[59] D. Whiteson,[29] D. A. Wijngaarden,[21] S. Willis,[37] S. J. Wimpenny,[33] J. Womersley,[35] D. R. Wood,[47] Q. Xu,[48] R. Yamada,[35] P. Yamin,[54] T. Yasuda,[35] Y. A. Yatsunenko,[22] K. Yip,[54] S. Youssef,[34] J. Yu,[58] M. Zanabria,[5] X. Zhang,[56] H. Zheng,[40] B. Zhou,[48] Z. Zhou,[41] M. Zielinski,[52] D. Zieminska,[39] A. Zieminski,[39] V. Zutshi,[37] E. G. Zverev,[24] and A. Zylberstejn[13]

(DØ Collaboration)

[1]*Universidad de Buenos Aires, Buenos Aires, Argentina*

[2]*LAFEX, Centro Brasileiro de Pesquisas Físicas, Rio de Janeiro, Brazil*

[3]*Universidade do Estado do Rio de Janeiro, Rio de Janeiro, Brazil*

[4]*Institute of High Energy Physics, Beijing, People's Republic of China*

[5]*Universidad de los Andes, Bogotá, Colombia*

[6]*Charles University, Center for Particle Physics, Prague, Czech Republic*

[7]*Institute of Physics, Academy of Sciences, Center for Particle Physics, Prague, Czech Republic*

[8]*Universidad San Francisco de Quito, Quito, Ecuador*
[9]*Institut des Sciences Nucléaires, IN2P3-CNRS, Universite de Grenoble 1, Grenoble, France*
[10]*CPPM, IN2P3-CNRS, Université de la Méditerranée, Marseille, France*
[11]*Laboratoire de l'Accélérateur Linéaire, IN2P3-CNRS, Orsay, France*
[12]*LPNHE, Universités Paris VI and VII, IN2P3-CNRS, Paris, France*
[13]*DAPNIA/Service de Physique des Particules, CEA, Saclay, France*
[14]*Universität Mainz, Institut für Physik, Mainz, Germany*
[15]*Panjab University, Chandigarh, India*
[16]*Delhi University, Delhi, India*
[17]*Tata Institute of Fundamental Research, Mumbai, India*
[18]*Seoul National University, Seoul, Korea*
[19]*CINVESTAV, Mexico City, Mexico*
[20]*FOM-Institute NIKHEF and University of Amsterdam/NIKHEF, Amsterdam, The Netherlands*
[21]*University of Nijmegen/NIKHEF, Nijmegen, The Netherlands*
[22]*Joint Institute for Nuclear Research, Dubna, Russia*
[23]*Institute for Theoretical and Experimental Physics, Moscow, Russia*
[24]*Moscow State University, Moscow, Russia*
[25]*Institute for High Energy Physics, Protvino, Russia*
[26]*Lancaster University, Lancaster, United Kingdom*
[27]*Imperial College, London, United Kingdom*
[28]*University of Arizona, Tucson, Arizona 85721*
[29]*Lawrence Berkeley National Laboratory and University of California, Berkeley, California 94720*
[30]*University of California, Davis, California 95616*
[31]*California State University, Fresno, California 93740*
[32]*University of California, Irvine, California 92697*
[33]*University of California, Riverside, California 92521*
[34]*Florida State University, Tallahassee, Florida 32306*
[35]*Fermi National Accelerator Laboratory, Batavia, Illinois 60510*
[36]*University of Illinois at Chicago, Chicago, Illinois 60607*
[37]*Northern Illinois University, DeKalb, Illinois 60115*
[38]*Northwestern University, Evanston, Illinois 60208*
[39]*Indiana University, Bloomington, Indiana 47405*
[40]*University of Notre Dame, Notre Dame, Indiana 46556*
[41]*Iowa State University, Ames, Iowa 50011*
[42]*University of Kansas, Lawrence, Kansas 66045*
[43]*Kansas State University, Manhattan, Kansas 66506*
[44]*Louisiana Tech University, Ruston, Louisiana 71272*
[45]*University of Maryland, College Park, Maryland 20742*
[46]*Boston University, Boston, Massachusetts 02215*
[47]*Northeastern University, Boston, Massachusetts 02115*
[48]*University of Michigan, Ann Arbor, Michigan 48109*
[49]*Michigan State University, East Lansing, Michigan 48824*
[50]*University of Nebraska, Lincoln, Nebraska 68588*
[51]*Columbia University, New York, New York 10027*
[52]*University of Rochester, Rochester, New York 14627*
[53]*State University of New York, Stony Brook, New York 11794*
[54]*Brookhaven National Laboratory, Upton, New York 11973*
[55]*Langston University, Langston, Oklahoma 73050*
[56]*University of Oklahoma, Norman, Oklahoma 73019*
[57]*Brown University, Providence, Rhode Island 02912*
[58]*University of Texas, Arlington, Texas 76019*
[59]*Texas A&M University, College Station, Texas 77843*
[60]*Rice University, Houston, Texas 77005*
[61]*University of Virginia, Charlottesville, Virginia 22901*
[62]*University of Washington, Seattle, Washington 98195*
[63]*Petersburg Nuclear Physics Institute, Gatchina, Russia*
(Received 19 July 2002; published 10 March 2003)

We present data on multiple production of jets with transverse energies near 20 GeV in $p\bar{p}$ collisions at $\sqrt{s}=1.8$ TeV. QCD calculations in the parton-shower approximation of PYTHIA and HERWIG and the next-to-leading order approximation of JETRAD are compared to the data for one, two, three, and four jet inclusive production. Transverse energy spectra and multiple jet angular and summed transverse-energy distributions are adequately described by the shower approximation while next-to-leading order calculations describe the data poorly.

DOI: 10.1103/PhysRevD.67.052001 PACS number(s): 14.65.Ha, 13.85.Ni, 13.85.Qk

I. INTRODUCTION

The study of multiple jet production at high transverse energy was a goal of the 1993–1995 run of the Fermilab Tevatron collider, and the results have been compared with leading-order QCD predictions by both the Collider Detector at Fermilab (CDF) [1] and DØ [2] Collaborations. These high-E_T data, where E_T is the transverse energy of the jet, are described satisfactorily by complete tree-level leading order $2\rightarrow N$ QCD calculations [3] and by the HERWIG parton-shower Monte Carlo [4] program. This kinematic region is described by $Q^2/\hat{s}\approx 1$, where Q^2 is the square of the momentum transfer between partons (which we set equal to E_T^2), and $\hat{s}$ is the square of the partonic center of mass energy. In this paper, we describe jet production measurements at significantly lower values of E_T where detailed measurement of jet production in this kinematic region can provide information on the evolution of higher-order jet processes. In the same low E_T region the DØ Collaboration has previously reported the ratio of the inclusive three-jet to the inclusive two-jet cross section as a function of the scalar sum of jet transverse energies ($H_T=\Sigma E_T$) with $E_T>$ 20 GeV [5]. The ratio data can be described by the JETRAD next-to-leading order Monte Carlo [6] program. In this paper we make comparisons between Monte Carlo data and several characteristics of multiple jet events including the leading jet transverse energy, the relative azimuthal angle between jets, and the summed vector transverse momenta of jets.

II. DATA SAMPLE AND CORRECTIONS

The data were collected with the DØ detector at a proton-antiproton center-of-mass energy $\sqrt{s}=1.8$ TeV. Jets were identified using the liquid-argon uranium calorimeters, which have segmentation of $\Delta\eta\times\Delta\phi=0.1\times 0.1$, where pseudorapidity $\eta=-\ln\tan\theta/2$, θ is the polar angle, and ϕ is azimuthal angle [7]. At least one calorimeter trigger tower ($\Delta\eta\times\Delta\phi=0.2\times 0.2$) with $E_T\geqslant 2$ GeV was required by a hardware trigger, and at least one jet with $E_T\geqslant 12$ GeV was required by a subsequent software trigger [8]. Jets were reconstructed using a fixed cone algorithm with radius $\Delta\mathcal{R}=\sqrt{\Delta\eta^2+\Delta\phi^2}=0.7$ in $\eta-\phi$ space [8]. The jet reconstruction threshold was $E_T=8$ GeV. If two jets overlapped and the shared transverse energy was more than 50% of the transverse energy of the lower-E_T jet, the jets were merged; otherwise they were split into two jets. The integrated luminosity of this data sample is 2.0 ± 0.3 nb^{-1}. Instantaneous luminosity was restricted to be below 3×10^{30} cm^{-2} s^{-1} to minimize the number of multiple $p\bar{p}$ interactions in a single beam crossing.

To provide events of high quality, online and offline selection criteria suppressed multiple interactions, the cosmic ray background, and spurious jets [8]. Jets were restricted to the pseudorapidity interval $|\eta|\leqslant 3$. The primary vertex of each event (reconstructed from time-of-flight as measured by scintillation counters [7]) was required to be within 50 cm of the detector center.

Jet energies have been corrected for calorimeter response, shower development, and various sources of noise [9]. These corrections constitute the largest source of systematic uncertainty on the jet cross section. Typical values of the jet energy correction are 15–30%, with an uncertainty of 2–4%. In our study, we consider jets with $E_T>20$ GeV; for an inclusive n-jet event, the n jets with the maximum E_T (the leading jets) must have transverse energy above the threshold value. For example, a 3-jet event must have at least 3 jets above 20 GeV. The trigger efficiency is 0.85 for the inclusive ($n=1$) jet sample for energies near threshold, rising rapidly to unity at larger E_T. The efficiency is essentially unity for $n>1$.

To compare with data, Monte Carlo (MC) events were generated using the PYTHIA 6.127 [10], HERWIG 5.9 [4], and JETRAD [6] programs. PYTHIA and HERWIG simulate particle-level jets in the parton-shower approximation. JETRAD simulates jets in the next-to-leading order approximation. To simulate detector resolution effects, the MC jet transverse energies were smeared with the experimentally determined jet energy resolution [9], which is $\approx$20% at $E_T=20$ GeV. Jet angular smearing used η and ϕ resolutions obtained by a MC simulation of the calorimeter response using HERWIG 5.9 and GEANT [11]. These resolutions are ≈ 0.08 at $E_T=20$ GeV. In PYTHIA and HERWIG, jets were reconstructed at the particle level using the DØ algorithm, and in JETRAD, at the parton level, using the Snowmass algorithm [12].

III. LEADING JET E_T DISTRIBUTIONS AND SYSTEMATIC UNCERTAINTIES

Distributions in transverse energy for the leading jet for inclusive $n=1$ to $n=4$ jet events are shown in Fig. 1, along

*Also at University of Zurich, Zurich, Switzerland.

†Also at Institute of Nuclear Physics, Krakow, Poland.

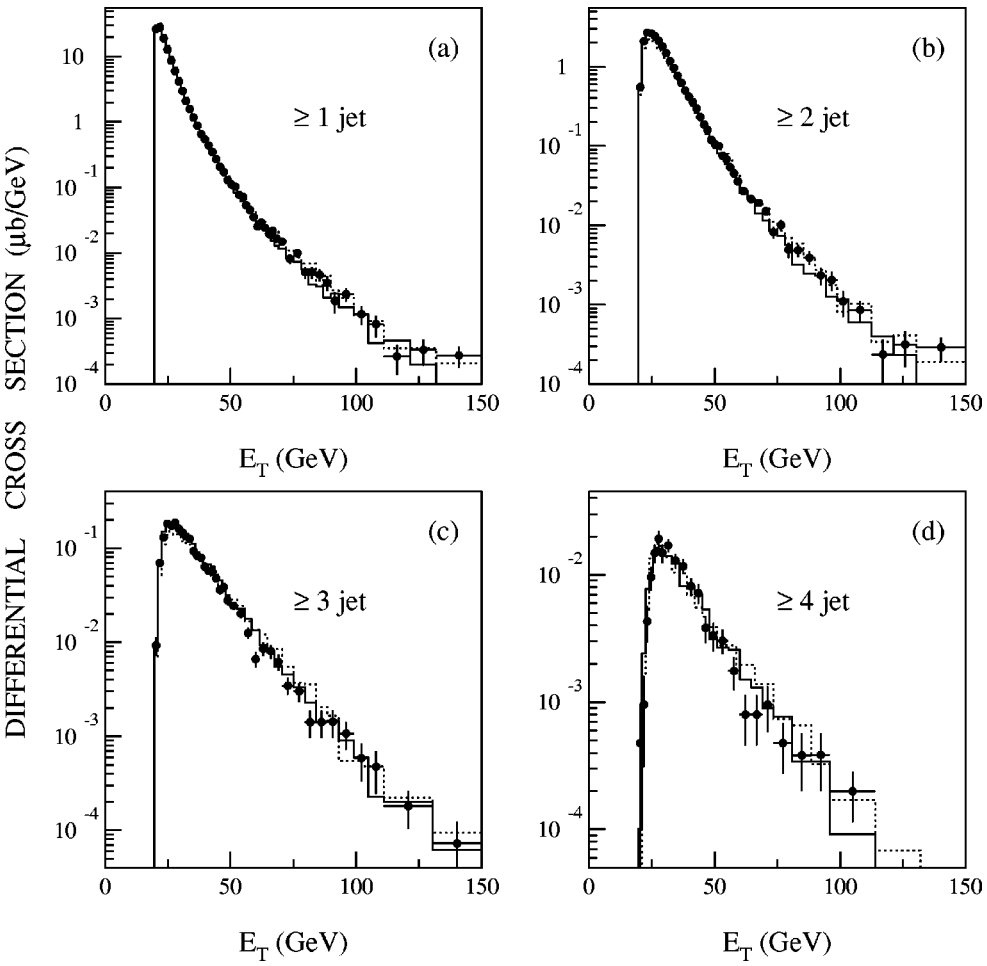

FIG. 1. The transverse energy distributions of the leading jet for (a) single-inclusive, (b) two-jet inclusive, (c) three-jet inclusive, and (d) four-jet inclusive events. Solid histograms show the PYTHIA simulation normalized (with a factor of 0.75) to the inclusive two-jet sample for $E_T > 40$ GeV. Dotted histograms are similarly normalized HERWIG results (increased by a factor of 1.6).

with the results from PYTHIA and HERWIG simulations. In these and all other plots, the data have been corrected for inefficiencies and energy calibration, but not for contributions from the underlying event. All simulated distributions have been smeared with energy and angular resolutions. Also to describe the data quantitatively, we normalize the theory (with a factor of 0.75 for PYTHIA and 1.6 for HERWIG) to the observed two-jet inclusive cross section in Fig. 1(b) for $E_T > 40$ GeV.

The normalized theory is in agreement with the data for all of the jet samples over the entire E_T interval. A detailed comparison is shown in Figs. 2 and 3. Here the simulations have been brought into agreement with the data by selecting parameters that enhance low E_T jet production. In the case of PYTHIA, the core of the hadronic matter distribution [10] has been increased to the fraction 0.32. An increased core fraction [the parameter PARP(83)] leads to enhancement of the multiple interaction rate [10], which tends to produce events with large multiplicity because of additional radiated low energy jets and underlying event energy. In the case of HERWIG, the minimum transverse momentum for the hard subprocesses has been set to 3.7 GeV. A decreased minimum transverse momentum (the parameter PTMIN) leads to increased soft underlying event contributions. The default values for these parameters are PARP(83)=0.5 and PTMIN $=10$ GeV. Variation of these values by more than 15% leads to disagreement with the low E_T data. Other parameters, when varied from their default values, do not change the distributions significantly.

Figures 2 and 3 show the fractional difference (Data $-$MC) / MC for the E_T spectra in Fig. 1 with the uncertainties arising from jet-energy calibration and resolutions. The systematic uncertainty on the cross section is due primarily to the uncertainty in the energy calibration. This uncertainty can be estimated by considering cross sections derived with ± 1 standard-deviation corrections to the jet energy scale. The same procedure can be used to derive the uncertainties due to jet energy and angular resolutions in the MC. At $E_T = 25$ GeV, the uncertainty in the three-jet cross section due to calibration of the data is 39%, and uncertainties in the MC due to energy and angular resolutions are 19% and 7%, respectively. The uncertainty from energy resolution represents the dominant uncertainty in the MC. In Figs. 2 and 3, the

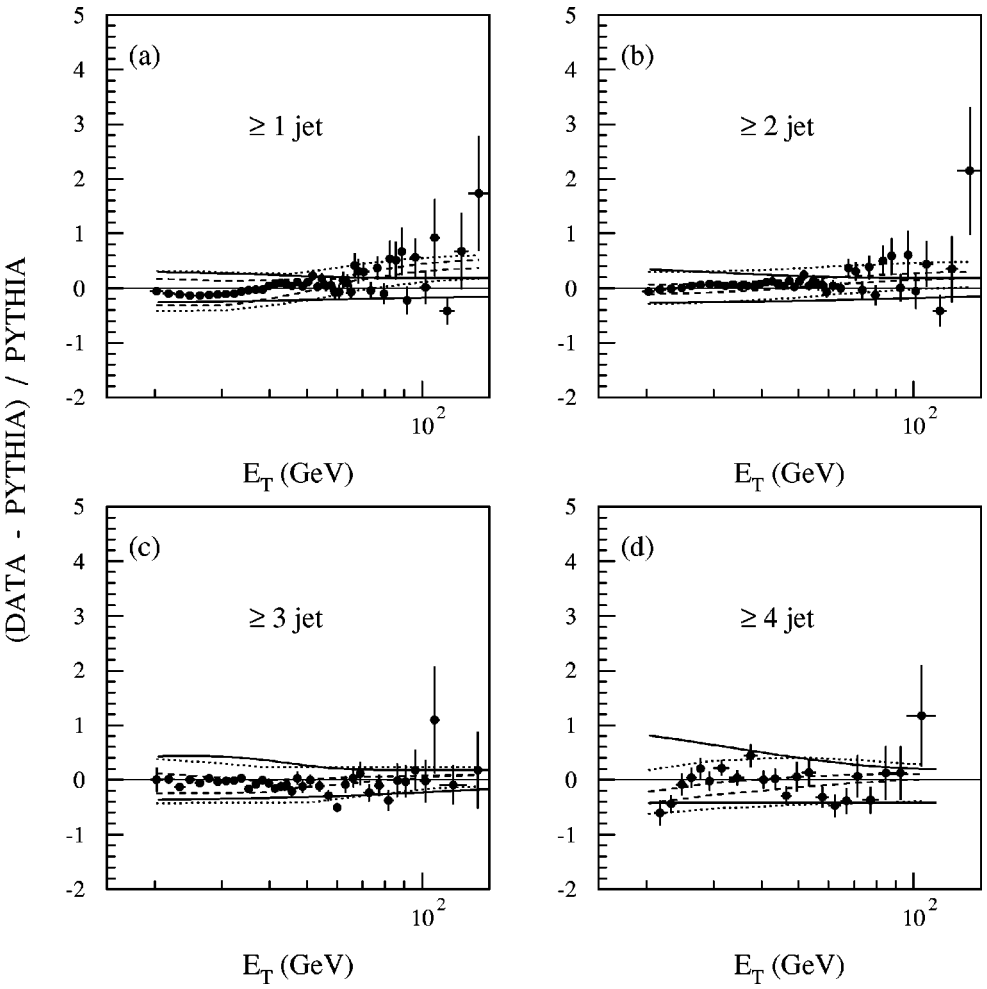

FIG. 2. (Data−PYTHIA)/PYTHIA as a function of the transverse energy of the leading jet for (a) single-jet inclusive, (b) two-jet inclusive, (c) three-jet inclusive, and (d) four-jet inclusive event samples. The relative systematic uncertainties in the cross section corresponding to the energy calibration added in quadrature with 15% uncertainty in luminosity are shown by the solid lines. The uncertainty in the ratio (Data − MC) / MC from energy and angle smearing is shown by the dashed lines. The total uncertainty on the ratio is shown by the dotted lines.

relative systematic uncertainties in the cross section corresponding to the energy calibration added in quadrature with 15% uncertainty in luminosity are shown by the solid lines. The uncertainty in the ratio (Data − MC) / MC from energy and angle smearing is shown by the dashed lines. The total uncertainty on the ratio is shown by the dotted lines. As shown in Figs. 2 and 3, both PYTHIA and HERWIG describe the data quite well.

IV. TRANSVERSE ENERGY AND AZIMUTHAL DISTRIBUTIONS

To explore features of three- and four-jet production, we turn to observations of relative azimuthal distributions, distributions in summed transverse momenta, and three-jet studies. In Fig. 4(a) we plot the azimuthal difference between the leading two jets in events with two or more jets. Figures 4(b)–4(d) show the azimuthal difference between the first and second, first and third, and second and third highest-E_T jets in three-jet events. In Fig. 4(a) we see the strong anticorrelation (in the transverse plane) expected of two-jet events. The peak of the distribution widens substantially in the three-jet sample [Figs. 4(b)–4(d)]. The peaks correspond to the kinematic constraint of transverse momentum conservation for jets produced in hard QCD subprocesses. PYTHIA (normalized as in Fig. 1) approximates the observed three-jet cross section and shapes. However, small discrepancies with HERWIG (also normalized as in Fig. 1) are evident.

Distributions of the square of the summed vector transverse momenta of jets $Q_T^2=(\mathbf{E}_{T1}+\mathbf{E}_{T2}+\cdots+\mathbf{E}_{Tn})^2$ in Fig. 5 show significant imbalance of the transverse momenta for n leading jets. If events at large Q_T^2 are removed by requiring balanced transverse energy, the corresponding three- and four-jet cross sections of Fig. 1 decrease at small E_T. The shoulder at $Q_T^2\approx 1600$ GeV^2 in Fig. 5(a) can be eliminated by restricting the event sample to just two jets with E_T above 20 GeV, and no other jets between 8 and 20 GeV. This shoul-

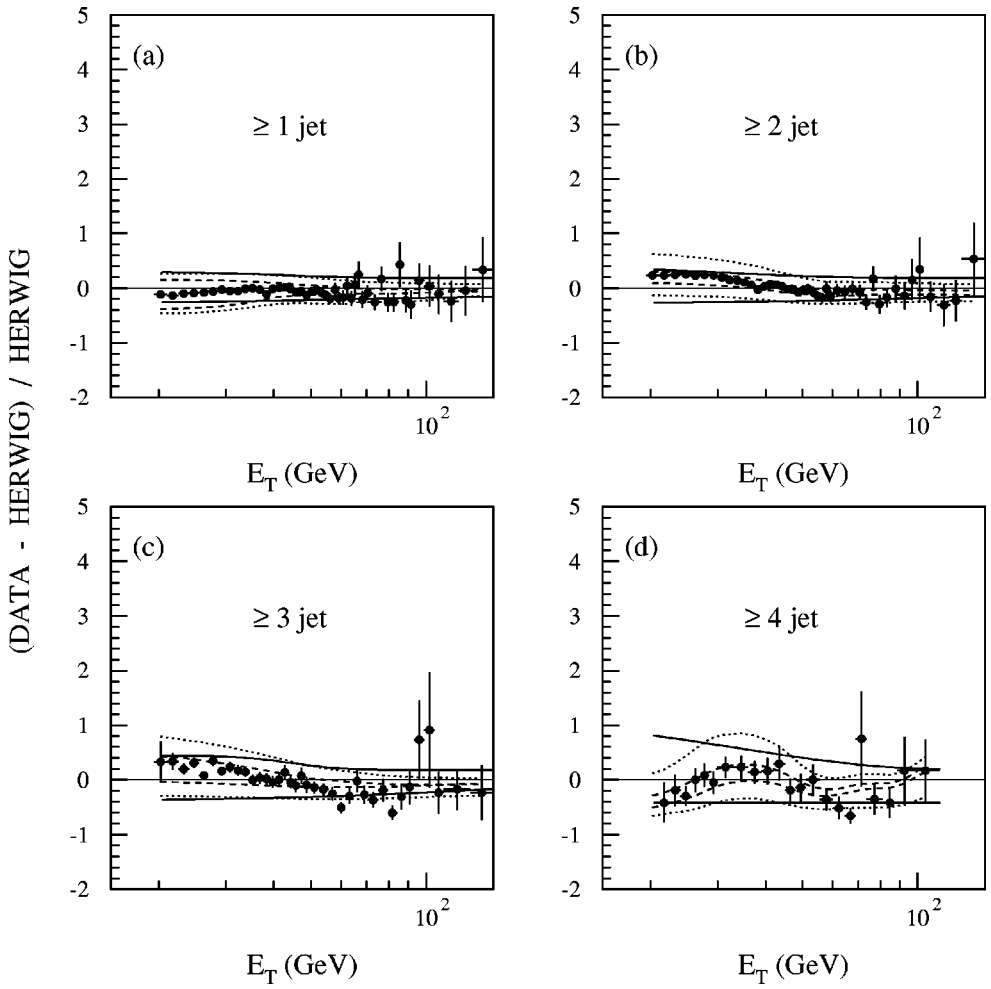

FIG. 3. (Data−HERWIG)/HERWIG as a function of the transverse energy of the leading jet for (a) single-jet inclusive, (b) two-jet inclusive, (c) three-jet inclusive, and (d) four-jet inclusive event samples. The relative systematic uncertainties in the cross section corresponding to the energy calibration added in quadrature with 15% uncertainty in luminosity are shown by the solid lines. The uncertainty in the ratio (Data−MC) / MC from energy and angle smearing is shown by the dashed lines. The total uncertainty on the ratio is shown by the dotted lines.

der can consequently be associated with higher-order radiation.

To find the pair of jets $\{i,j\}$ most likely to originate from the hard interaction (rather than from gluon bremsshtrahlung), we define the scaled summed dijet vector transverse momentum: $\mathbf{q}_{ij}=(\mathbf{E}_{Ti}+\mathbf{E}_{Tj})/(E_{Ti}+E_{Tj})$. We choose the pair with the smallest magnitude of this vector and in Figs. 6(a) and 7(a) plot the distribution of the relative azimuthal angle Φ_c between the jets in that pair. The data, PYTHIA, and HERWIG show a narrow maximum in the region where two jets from the hard scatter appear back-to-back ($\Phi_c=\pi$). The prediction from JETRAD is peaked away from $\Phi_c\approx\pi$ because only one extra jet is present.

Figures 6(b) and 6(c) and Figs. 7(b) and 7(c) show the azimuthal separation of the third jet from each of the two jets that correspond to the minimum q_{ij}^2. These distributions contain events only for $\pi-\Phi_c\leqslant 0.4$; that is, events in which the balanced jets are essentially back-to-back. If the third jet were correlated with the balanced jets, it would be observed nearby or opposite the balanced jets. However, the data show the third jet to be weakly correlated with the balanced jets, and emitted at all angles. The uncertainties associated with energy calibration and luminosity are shown by the solid lines in Figs. 6 and 7. Uncertainties from the energy resolution are shown by dashed lines in Fig. 6.

We see that the data, PYTHIA, and HERWIG have wider distributions than JETRAD. PYTHIA describes the data quite well, while JETRAD fails. The agreement with PYTHIA has been achieved only with enhanced multiple parton interaction rates. HERWIG demonstrates small qualitative disagreement with the shape of the azimuthal plot of Fig. 7(b); the peak at $\pi/2$ is produced by jets reconstructed from the underlying-event energy [4] and grows quickly with small changes in PTMIN. Such jets are strongly overlapped with more than one jet. If jets overlapping two or more nearby jets are excluded, the HERWIG shape in Fig. 7(b) improves but the agreement shown in Fig. 7(a) worsens. (The cone algorithm reconstructs jets from seed towers and may therefore recon-

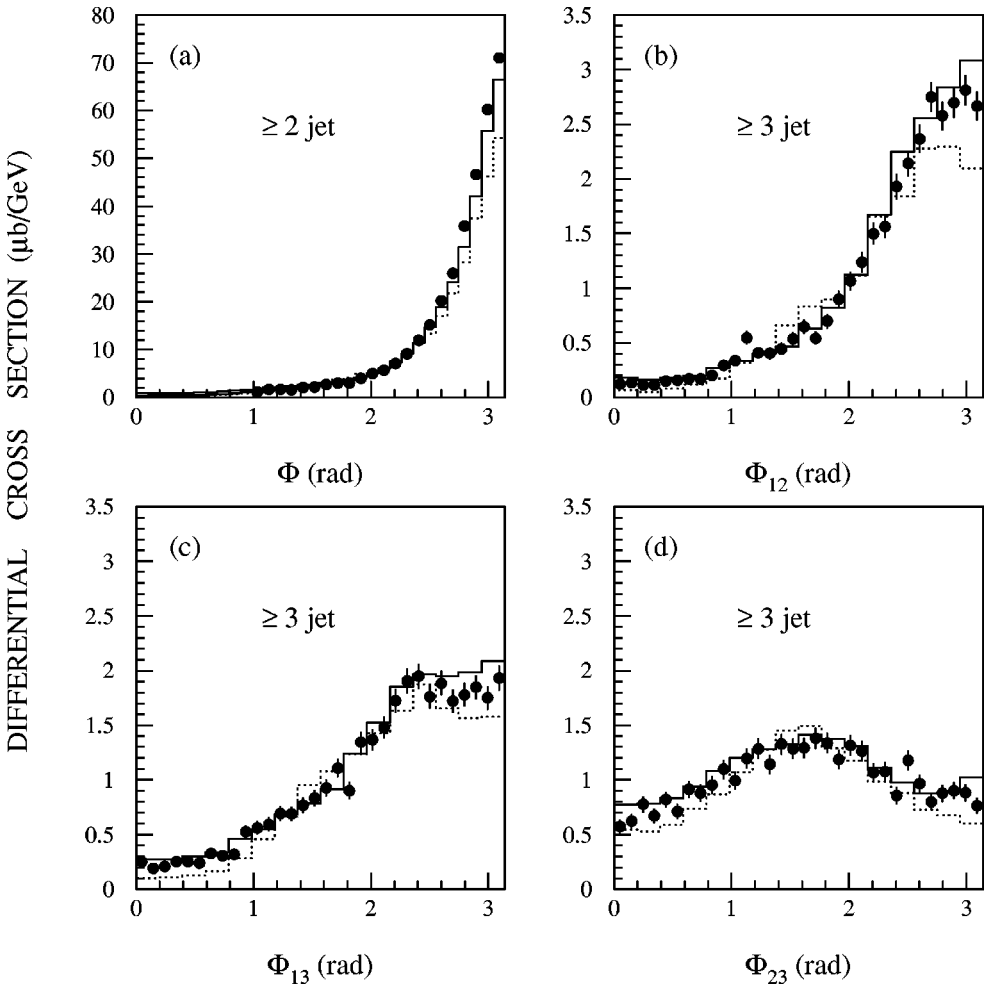

FIG. 4. Distributions of the relative azimuthal angle between two jets in (a) two-jet inclusive events and in three-jet inclusive events [(b)–(d)]. Jets are ordered by their transverse energies. The PYTHIA predictions are indicated by the solid histograms and the HERWIG predictions by the dotted histograms.

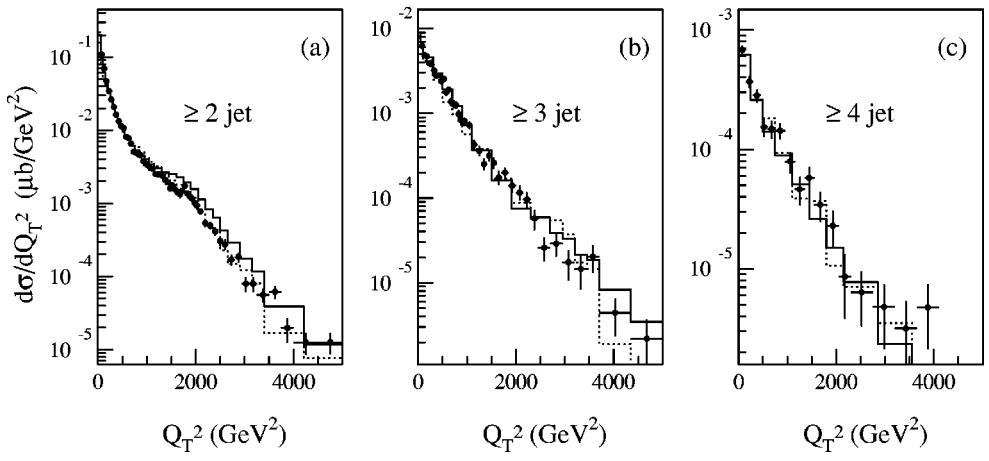

FIG. 5. Distributions of the square of the summed vector transverse momenta Q_T^2, for (a) two-jet inclusive, (b) three-jet inclusive, and (c) four-jet inclusive event samples. The PYTHIA predictions are indicated by the solid histograms and the HERWIG predictions by the dotted histograms.

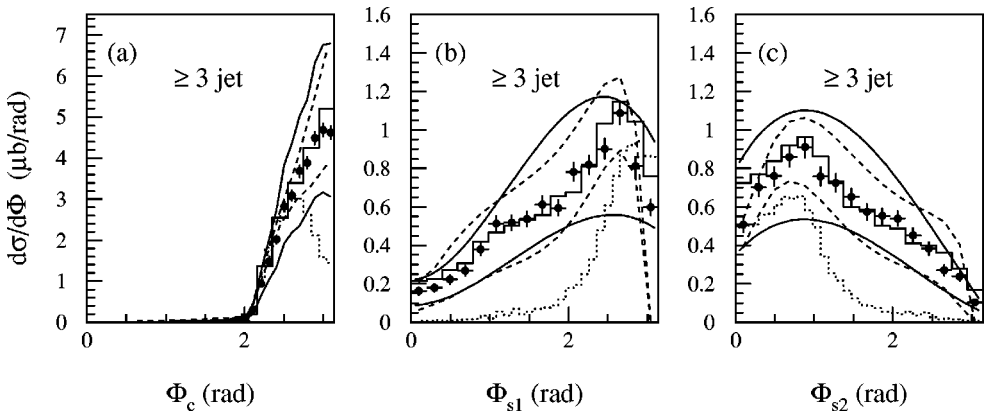

FIG. 6. Azimuthal distributions between the leading jets in 3-jet events. The data is shown by the closed circles. Panel (a) shows the azimuthal separation between the two jets with the minimum summed transverse energy. Panel (b) shows the azimuthal separation between the third leading jet and the first jet of the minimum transverse energy pair. Panel (c) shows the azimuthal separation between the third leading jet and the second jet of the pair. PYTHIA is given by the solid histograms, JETRAD is shown by the dotted histograms. The uncertainties associated with energy calibration and luminosity are shown by the solid lines. Uncertainties from the energy resolution are shown by dashed lines.

struct jets sharing energy. The reconstruction algorithm then merges or splits the energy encompassed in these overlapping jets [8].) Elimination of these jets tends to suppress contributions from the soft underlying event. Soft interactions result in a wide distribution of particles throughout angular phase space. Jets reconstructed from these particles tend to be wider and of lower energy than more collimated partonic jets. Such jets often share a significant fraction of energy with similar, neighboring jets and are merged into a single jet.

The shapes of the simulated distributions are sensitive to modeling of the multiple parton interactions. Tuning of the multiple interaction contribution in PYTHIA and the minimum generated transverse momentum in HERWIG are required for good agreement. In particular, simulations with smaller contributions from soft parton interactions show discrepancies with the data.

V. CONCLUSIONS

In this paper we showed comparisons between Monte Carlo calculations and data for several characteristics of multiple jet events with a low jet-E_T threshold. These comparisons included the leading jet transverse energy, the relative azimuthal angle between jets, and the summed vector transverse momenta of jets. Our data on multiple jet production at low E_T agree with PYTHIA and HERWIG. This is observed in the distributions of the transverse energy of the leading jets (Fig. 1), azimuthal distributions (Fig. 4), in the square of the summed vector transverse momenta Q_T^2 (Fig. 5), and in the three-jet angular distributions that suggest the presence of a weakly correlated jet (Figs. 6 and 7). JETRAD cannot adequately describe the angular distributions of the three leading jets in three jet events.

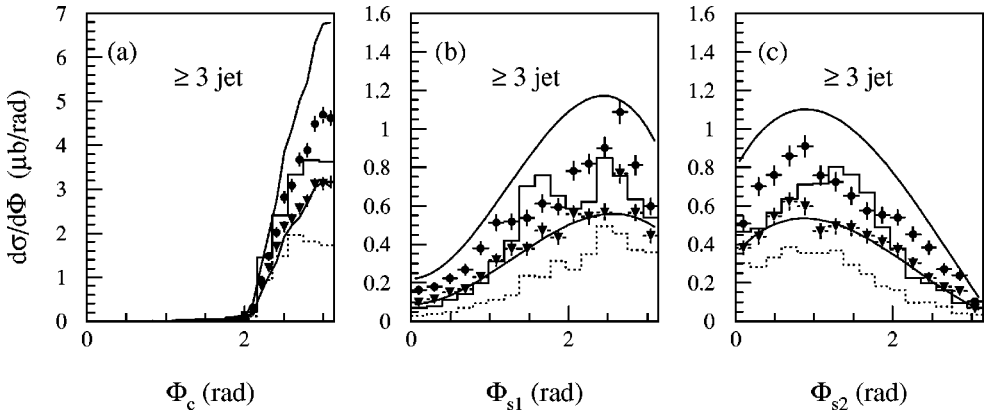

FIG. 7. Azimuthal distributions between the leading jets in 3-jet events. The data is given by the closed circles (all jets) and by the closed triangles (the jets overlapped with more than one jet are excluded). Panel (a) shows the azimuthal separation between the two jets with the minimum summed transverse energy. Panel (b) shows the azimuthal separation between the third leading jet and the first jet of the minimum transverse energy pair. Panel (c) shows the azimuthal separation between the third leading jet and the second jet of the pair. HERWIG is given by the solid histograms (all jets), and the dotted histograms (the jets overlapped with more than one jet are excluded). The uncertainties associated with energy calibration and luminosity are shown by the solid lines.

ACKNOWLEDGMENTS

We thank the staffs at Fermilab and collaborating institutions, and acknowledge support from the Department of Energy and National Science Foundation (USA), Commissariat à L'Energie Atomique and CNRS/Institut National de Physique Nucléaire et de Physique des Particules (France), Ministry for Science and Technology and Ministry for Atomic Energy (Russia), CAPES and CNPq (Brazil), Departments of Atomic Energy and Science and Education (India), Colciencias (Colombia), CONACyT (Mexico), Ministry of Education and KOSEF (Korea), CONICET and UBACyT (Argentina), The Foundation for Fundamental Research on Matter (The Netherlands), PPARC (United Kingdom), Ministry of Education (Czech Republic), A. P. Sloan Foundation, and the Research Corporation.

[1] CDF Collaboration, F. Abe *et al.*, Phys. Rev. Lett. **75**, 608 (1995).
[2] DØ Collaboration, S. Abachi *et al.*, Phys. Rev. D **53**, 6000 (1996).
[3] F.A. Berends and H. Kuijf, Nucl. Phys. **B353**, 59 (1991); F.A. Berends, W.T. Giele, and H. Kuijf, *ibid.* **B333**, 120 (1990); Phys. Lett. B **232**, 266 (1990).
[4] G. Marchesini and B. Webber, Nucl. Phys. **B310**, 461 (1988); G. Marchesini *et al.*, Comput. Phys. Commun. **67**, 465 (1992).
[5] DØ Collaboration, B. Abbott *et al.*, Phys. Rev. Lett. **86**, 1955 (2001).
[6] W.T. Giele, E.W.N. Glover, and David A. Kosower, Nucl. Phys. **B403**, 633 (1993); Phys. Rev. Lett. **73**, 2019 (1994).
[7] DØ Collaboration, S. Abachi *et al.*, Nucl. Instrum. Methods Phys. Res. A **338**, 185 (1994).
[8] DØ Collaboration, B. Abbott *et al.*, Phys. Rev. D **64**, 032003 (2001).
[9] DØ Collaboration, B. Abbott *et al.*, Phys. Rev. Lett. **86**, 1707 (2001).
[10] T. Sjostrand, Comput. Phys. Commun. **82**, 74 (1994).
[11] R. Brun and F. Carminati, CERN Program Library, Long Writeup W5013, 1993.
[12] J. Huth *et al.*, in *Proceedings of Research Directions for the Decade, Snowmass, 1990*, edited by E. L. Berger (World Scientific, Singapore, 1992).